

## GREEN SYNTHESIS AND CHARACTERIZATION OF TiO<sub>2</sub> NANOPARTICLES USING *Lonchocarpus cyanescens*

Adamu Saidu<sup>1,2\*</sup>, Nasirudeen Mohammed Baba<sup>2</sup> and Timothy Akpomie<sup>2</sup>

<sup>1</sup>Department of Chemistry, Federal University of Technology Owerri, Nigeria

<sup>2</sup>Department of Chemistry, Federal University of Lafia, Nigeria

\*Corresponding email: [hamdaansaid1@gmail.com](mailto:hamdaansaid1@gmail.com)

### ABSTRACT

This study describes the synthesis of titanium dioxide (TiO<sub>2</sub>) nanoparticles using green techniques with *Lonchocarpus cyanescens* extract as a sustainable, non-toxic, and cost-effective alternative to conventional chemical methods. The optical, functional, and morphological properties of the synthesized TiO<sub>2</sub> nanoparticles were characterized using UV-Visible spectroscopy, Fourier Transform Infrared (FTIR) spectroscopy, X-ray diffraction (XRD) and Scanning Electron Microscopy (SEM). The green-synthesized TiO<sub>2</sub> nanoparticles' FTIR spectrum showed a prominent absorption band at 1024 cm<sup>-1</sup>, which corresponds to C–O stretching vibrations commonly found in alcohols, carboxylic acids, esters, and ethers; additionally, peaks at 1024 and 493 cm<sup>-1</sup> were attributed to Ti–O stretching and Ti–O–Ti bridging vibrations, respectively; the clear peak at 493 cm<sup>-1</sup> verified the successful formation of TiO<sub>2</sub> nanoparticles. The optical band gap of the synthesised nanoparticles was examined using UV-Visible spectroscopy, demonstrating the efficacy of the green synthesis approach in developing optically active TiO<sub>2</sub> nanomaterials. The photo absorption characteristics of TiO<sub>2</sub> nanoparticles was analysed across a wavelength range of 200–800 nm. The results exhibited a prominent absorption peak at 225 nm with an absorbance below 1, confirming the successful synthesis of pure TiO<sub>2</sub> nanoparticles. The surface morphological studies of the TiO<sub>2</sub> nanoparticles was carried out using (SEM) and it reveals that the synthesized TiO<sub>2</sub> particles were in spherical in shape and aggregated into an irregular structure. The X-ray diffraction (XRD) pattern of TiO<sub>2</sub> nanoparticles indicates that the calculated average crystallite size for pure TiO<sub>2</sub> is around 12.9 nm.

**Keywords:** Nanoparticles, Crystallite, Absorption, Band gap, *Lonchocarpus cyanescens*

### INTRODUCTION

Nanoparticles are of major consideration because of their extremely small size and large surface-to-volume ratio. These will give nanoparticles some unique and superior properties both physically and chemically in comparison to their bulk composition (Iravani, 2011). Many important technologies utilizing nanoscale structures (nanoparticles) in the fields of optics, electronics, biomedical science, mechanics, drug-gene delivery, chemical industry, optoelectronic devices, nonlinear optical devices, catalysis, space industries, energy science, and photoelectrochemical applications rely heavily on nanotechnology (Singh *et al.*, 2019). Because of their affordability and energy efficiency, green synthesis techniques are becoming more, and more popular in chemistry and chemical technology. By removing the need for toxic reagents and lowering production costs and energy consumption, green technologies provide a safer and more sustainable alternative to conventional methods that rely on dangerous chemical agents like sodium borohydride or hydrazine. TiO<sub>2</sub> was an excellent photocatalyst due to the oxidizing strength of the photogenerated holes, its chemical inertness, and its non-toxicity. TiO<sub>2</sub> have tremendous advantages in solar energy transferring and photocatalysis of poison compounds in environment (Rauwel *et al.*, 2015).

Titanium dioxide (TiO<sub>2</sub>) has three primary crystalline phases: anatase, rutile, and brookite. Brookite has an orthorhombic crystal structure, unlike anatase and rutile, which have tetragonal structures. TiO<sub>2</sub> nanoparticles are typically analysed using X-ray diffraction (XRD), scanning electron microscopy (SEM), and ultraviolet-visible spectroscopy (UV-Vis) (Rauwel *et al.*, 2015). The development of effective environmental remediation procedures has sparked an interest in eco-friendly synthesis processes. Titanium dioxide (TiO<sub>2</sub>) nanoparticles can be synthesised using several processes, such as hydrothermal, solvothermal, microwave-assisted, and ultrasonication.

However, these traditional procedures frequently rely on toxic reducing and stabilising chemicals, and are typically considered less sustainable and environmentally benign than green synthesis methods, which use natural resources and safer protocols (Raveendran *et al.*, 2003). TiO<sub>2</sub> nanoparticles' unique characteristics and applications in several industries have led to substantial research in recent years. Apart from its well-known photocatalytic activity, TiO<sub>2</sub> has various notable applications in light guides, solar cells, hydrogen storage, and bio-application which can be optimised at the nanoscale (Smith *et al.*, 2006). Particularly nanostructured TiO<sub>2</sub>, with its high specific surface area to volume ratio, enables improvements in

gas-sensing processes or catalysis. This study fills a gap by generating green-synthesized TiO<sub>2</sub> nanoparticles from *Lonchocarpus cyanescens* leaves to cancel out, high energy and high production cost involved in the usual routes of synthesizing nanoparticles via the conventional techniques of using hazardous chemicals like hydrazine and sodium borohydride.

### Titanium Dioxide (TiO<sub>2</sub>) Nanoparticles

TiO<sub>2</sub> nanoparticles are among the most extensively produced metal oxide nanoparticles, owing primarily to their respectable and diverse features derived from the physical, chemical stability, optical, and electrical. Anatase (tetragonal,  $a = b = 3.782 \text{ \AA}$ ,  $c = 9.502 \text{ \AA}$ ), brookite (rhombohedral,  $a = 5.436 \text{ \AA}$ ,  $b = 9.166 \text{ \AA}$ ,  $c = 5.135 \text{ \AA}$ ), and rutile (tetragonal,  $a = b = 4.854 \text{ \AA}$ ,  $c = 2.953 \text{ \AA}$ ) are its different mineral forms, but generally, TiO<sub>2</sub> exists in the former one due to enhanced photocatalytic activity. Attempts were made for the green synthesis of TiO<sub>2</sub> nanoparticles owing to its photocatalytic importance (Peralta-Videa *et al.*, 2016). The rutile phase of titanium dioxide (TiO<sub>2</sub>) is the most stable crystalline form, according to thermodynamics. In all three polymorphs (anatase, rutile, and brookite), each titanium ion is coordinated by six oxygen ions, resulting in a deformed octahedral geometry.

However, the extent of edge-sharing between adjacent octahedra varies: rutile shares two edges, brookite shares three, and anatase shares four, influencing their structural stability and physical properties (Godbert *et al.*, 2018). In rutile TiO<sub>2</sub>, the two axial oxygen atoms are the furthest from the titanium ion, while in anatase, the surrounding oxygen atoms are closer to the core titanium ion. Rutile has Ti-O bond lengths of around 2.01 Å and 1.92 Å, while anatase has somewhat shorter lengths of 1.95 Å and 1.91 Å, respectively. Anatase and rutile are the most investigated and published forms of TiO<sub>2</sub> in the scientific literature due to their significant physicochemical features and uses. Titanium dioxide (TiO<sub>2</sub>) has been synthesised in different forms, such as nanotubes, crystals, nanorods, powders, and thin films. Liquid phase processing is one of the most extensively used chemical synthesis procedures due to its ease and adaptability. This process has various advantages, including accurate stoichiometric control, the manufacture of homogeneous materials, and the capacity to build complicated geometries and composite structures. Despite these advantages, liquid phase synthesis has some drawbacks, such as the use of expensive precursors, longer processing durations, and the possibility of carbon contamination in the finished product (Periyat *et al.*, 2008).

Hudlikar *et al.* (2012) shown that TiO<sub>2</sub> nanoparticles were synthesized by the reaction between latex of *Jatropha curcas* leaf and TiO(OH)<sub>2</sub>. According to the XRD, the synthesised TiO<sub>2</sub> nanoparticles were characterized in 100–200 nm size. Using an aqueous extract of dried clove buds (*Syzygium aromaticum*), Raghunandan *et al.*, (2010) reported the rapid extracellular synthesis of gold nanocrystals, with the formation of nanoparticles occurring within minutes. X-

ray diffraction (XRD) analysis confirmed the crystalline nature of the synthesised particles, while Fourier Transform Infrared Spectroscopy (FTIR) was used to investigate the potential biochemical mechanisms involved in the biosynthesis process. The study identified flavonoids present in clove buds as key agents responsible for the bioreduction of gold ions and the stabilisation of nanoparticles, with the resulting colloidal solution exhibiting stability for more than six weeks.

Sundrarajan and Gowri (2011), used a green method for preparing titanium dioxide (TiO<sub>2</sub>) nanoparticles by reacting titanium tetra isopropoxide with an ethanolic leaf extract of *Nyctanthes arbortristis*. Nanoparticles were obtained by constantly stirring the reaction mixture at 50°C for four hours and then calcining it at 500°C. SEM, XRD, and particle size analysis were used to characterise the synthesised TiO<sub>2</sub> material. The results showed a typical grain size of about 100 nm. SEM analysis revealed TiO<sub>2</sub> nanoparticles had a spherical shape with an average particle size of 100 to 150 nm.

## MATERIALS AND METHODS

### Experimental

#### Materials

The *Lonchocarpus cyanescens* (Fig. 1) leaves were locally obtained at Umuanu. The area lies approximately within the latitude range of 5.4°N and longitude range of 6.9°E, Owerri West Local Government Area, Imo State Nigeria. The leaves were washed and air dried for a week. The dried leaves were then powdered using pestle and mortar and sieved through 2mm sieve. They were kept in a polythene bag prior to analysis. 10g of powdered *L. cyanescens* leaf was weighed and transferred into 250 ml volumetric flask. 100 ml of the solvent (distilled water) was added. The mixture was kept for 24h. For the synthesis of titanium dioxide nanoparticles the extract was filtered using Whatmann filter Paper No.1 (Subhapiya & Gomathipriya, 2018).



Figure 1: *Lonchocarpus cyanescens*

### Green Synthesis of Pure Titanium Dioxide (TiO<sub>2</sub>)

The TiO<sub>2</sub> nanoparticles synthesis was carried out by adding 4ml of Titanium isopropoxide in a drop wise under constant stirring at moderate speed into a beaker

containing 40ml of *Lonchocarpus cyanescens* extract and the pH was measured to be 2.0 and was used without further adjustment. After stirring for 2h, particles were formed, afterwards the particle were separated using Whatmann filter paper No.1 and the precipitate obtained was washed with distilled water repeatedly to remove the unwanted ions. The precipitate was dried at 80°C for 2h and calcined at 450°C for 2h. The final yield of the nanopowder was white precipitate (Kandregula, 2015).

### Characterizations

A combination of analytical techniques, including Fourier Transform Infrared Spectroscopy (FTIR), UV-Visible spectroscopy, Scanning Electron Microscopy (SEM), and X-ray Diffraction (XRD), were used to characterise the synthesised titanium dioxide (TiO<sub>2</sub>) nanoparticles. FTIR analysis was used to identify functional groups and bioactive compounds associated with the plant-mediated synthesis, which provided insights into the chemical interactions involved in nanoparticle formation. UV-Visible spectroscopy was used to confirm the successful synthesis of TiO<sub>2</sub> nanoparticles via the green synthesis route, including their optical properties and formation using reduction methods based on plant extract. SEM was carried out to provide a clear image of TiO<sub>2</sub> nanoparticles. XRD was utilized to investigate the crystalline of the materials and offer details on unit cell dimensions. Using an X-ray diffractometer Rigaku Mini Flex Instrument Cu K radiation (= 1.5418, 30 kV, 30 mA) and a scanning speed of 0.01 to 100°/min.

### RESULTS AND DISCUSSION

As shown in the Fig. 2, the presence of hydroxyl groups on the nanoparticle surface is thought to play a crucial role in enhancing the photocatalytic activity of the TiO<sub>2</sub> nanoparticles by facilitating the generation of reactive oxygen species under light irradiation. The FTIR spectra of the green-synthesized TiO<sub>2</sub> nanoparticles were analysed to identify the functional groups involved in the formation and stabilisation of the nanoparticles. A broad absorption band at 3354 cm<sup>-1</sup> was observed, which corresponds to the O–H stretching vibrations of hydroxyl groups, while a smaller peak at 1628 cm<sup>-1</sup> was associated with surface-adsorbed water molecules. The green-synthesized TiO<sub>2</sub> nanoparticles' FTIR spectrum also showed a clear absorption band at 1024 cm<sup>-1</sup>, which corresponds to C–O stretching vibrations. These vibrations are suggestive of the presence of alcohols, carboxylic acids, esters, and ethers, which are probably the result of phytochemicals in the root extract. Furthermore, Ti–O stretching and Ti–O–Ti bridging vibrations were identified as the causes of the bands at 1024 and 493 cm<sup>-1</sup>, respectively. Notably, the noticeable peak at 493 cm<sup>-1</sup> confirms the successful synthesis using the green technique and acts as a confirmatory signature of TiO<sub>2</sub> nanoparticle development (Sethy *et al.*, 2020).

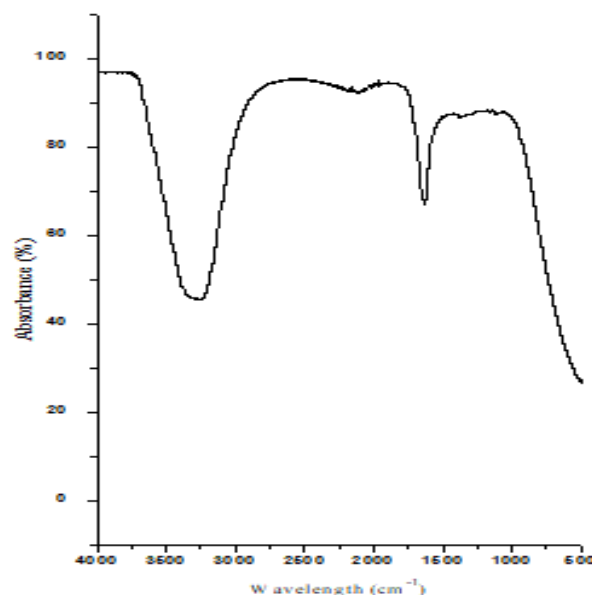


Figure 2: FT-IR of TiO<sub>2</sub> nanoparticles

Table 1: UV-visible absorbance values

Wavelength (nm)	Absorbance	hν (eV)	Ahν	(ahν) <sup>1/2</sup>
320	0.251	3.875	0.973	0.986
330	0.253	3.758	0.951	0.975
340	0.253	3.647	0.923	0.960
350	0.255	3.543	0.903	0.950
360	0.251	3.444	0.865	0.930
370	0.252	3.351	0.844	0.919
380	0.249	3.263	0.812	0.901
390	0.247	3.179	0.785	0.886
400	0.243	3.100	0.753	0.868
420	0.237	2.952	0.700	0.837

### UV-Visible Spectroscopy

The band gap of green route-synthesised TiO<sub>2</sub> nanoparticles was investigated to be 3.2 eV using the Tauc relation for an indirect allowed transition by plotting (ahν)<sup>1/2</sup> versus hν from the UV-Visible absorbance values as shown in Fig. 3 and Table 1. The photo absorption characteristic of TiO<sub>2</sub> nanoparticles was analyzed across a wavelength range of 200–800 nm. As presented in Fig. 3, the results exhibited a prominent absorption peak at 225 nm with an absorbance below 1, confirming the successful synthesis of green TiO<sub>2</sub> nanoparticles (Nadaroğlu *et al.*, 2017). This is attributed to the charge transfer transition from O<sup>2-</sup> (2p) to Ti<sup>4+</sup> (3d) orbitals. This shift also attributed to the quantum size effect, where reduction in particle size leads to an increase in band gap energy. Although bulk TiO<sub>2</sub> typically exhibits an adsorption edge around 320 – 380 nm, several studies have reported that TiO<sub>2</sub> nanoparticles can display adsorption maxima within 200 – 300 nm region, particularly for smaller particles sizes and green synthesized systems (Sellami *et al.*, 2025).

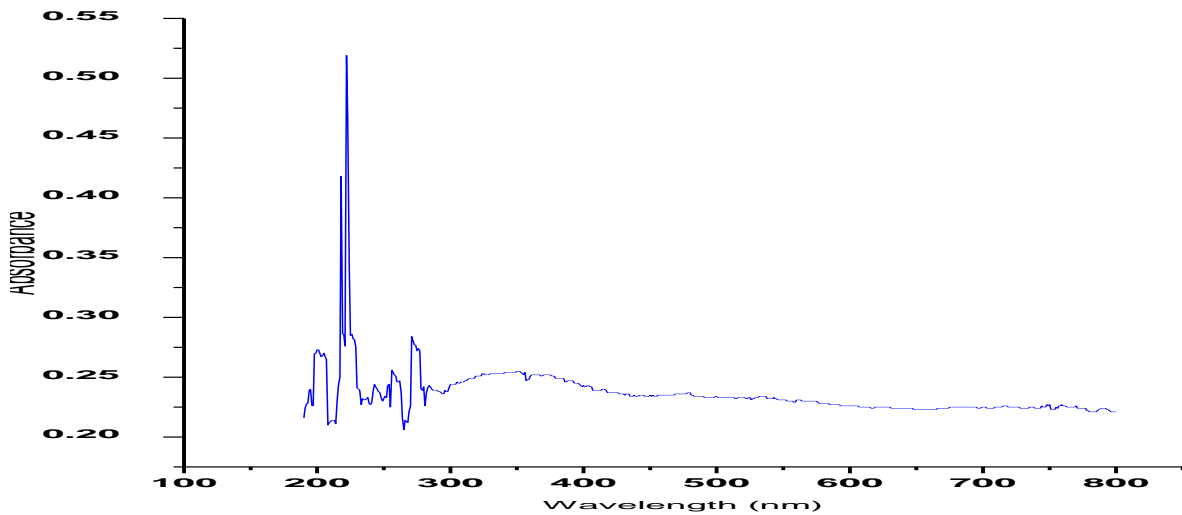


Figure 3: UV visible of TiO<sub>2</sub> nanoparticles

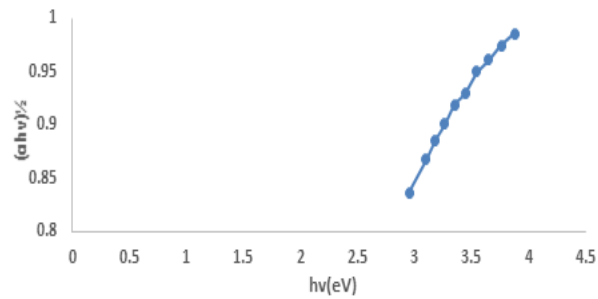


Figure 4: Tau plot of TiO<sub>2</sub> nanoparticles

**SEM Image of TiO<sub>2</sub> Nanoparticles**

The surface morphological studies of the TiO<sub>2</sub> nanoparticles synthesized was carried out using Scanning Electron Microscopy (SEM). As can be seen in Fig. 5, the produced TiO<sub>2</sub> nanoparticles had a spherical shape with a particle diameter of about 1-18 μm and the average particle size of 8.3 μm (8300 nm). Because of their high surface energy and propensity to minimise surface area, nanoparticles often agglomerate into irregular clusters, and a small agglomeration of the powder was also observed (Anbuvaran *et al.*, 2025).



Figure 5: SEM image of TiO<sub>2</sub>

### XRD Pattern of TiO<sub>2</sub> Nanoparticles

The synthesized TiO<sub>2</sub> nanoparticles XRD pattern as shown in Fig. 6 indicates its crystalline nature. There were notable peaks in 2θ range at 25.5°, 37°, 38°, 53° and 62°, which correspond to planes 101, 004, 200, 105, and 204 respectively which are characteristics of TiO<sub>2</sub> mineral with anatase phase according to JCPDS card of TiO<sub>2</sub>. The calculated average crystallite size for pure TiO<sub>2</sub> nanoparticles was approximately 12.9 nm calculated by Scherer's formula;

$$D = \frac{K\lambda}{\beta \cos\theta}$$

Where: D = crystallite size; K = shape factor; λ = X-ray wavelength; β = full width at half maximum (FWHM) in radians; θ = Bragg angle

**Table 2: FWHM value**

2θ (°)	FWHM (°)	β (rad)
25.5	0.60	0.0105
37.0	0.70	0.0122
38.0	0.72	0.0126
53.0	0.80	0.0140
62.0	0.85	0.0148

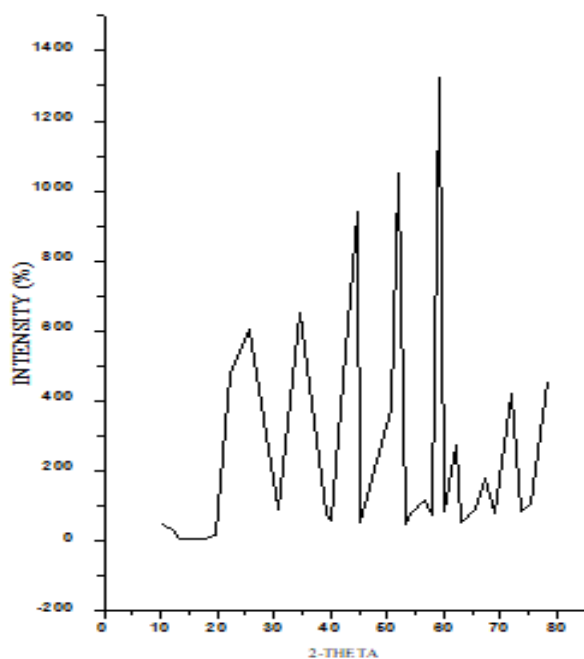


**Figure 6: XRD pattern of TiO<sub>2</sub> nanoparticles**

The absence of peaks at 27.4° and 36.1° 2θ suggests minimal rutile content, indicating phase purity in favour of anatase. This phase identification implies that the synthesized TiO<sub>2</sub> nanoparticles possess a predominantly anatase structure, which is preferable for photocatalytic applications due to its high surface activity and stability (Nainani *et al.*, 2012).

### CONCLUSION

*Lonchocarpus cyanescens* leaves extract was utilised to synthesise TiO<sub>2</sub> nanoparticles using a green technique, and the generated nanoparticles were characterised to

evaluate their physical, chemical, structural, and morphological behaviour. The size of the TiO<sub>2</sub> nanoparticles was successfully controlled in this work using the green synthesis method. With an average particle size of roughly 12.9 nm, the resultant nanoparticles had a spherical shape and aggregated into irregular clusters. FT-IR, UV-VIS, SEM and XRD pattern confirms the successful synthesis of TiO<sub>2</sub> nanoparticles, most likely in the anatase phase, with high phase purity and nanoscale crystallite size. These properties make them ideal for applications in wastewater treatment and photocatalysis due to enhanced surface area and reactivity.

**Conflict of interest:** The authors declare no conflict of interest.

### REFERENCES

- Anbuvaran, M., Vinosel, M. V., Dhatshanamurthi, P., Rajesh, S., Ramesh, M. and Kannadasan, N. (2025). Investigation of pure TiO<sub>2</sub> and BaO-Loaded TiO<sub>2</sub>nanocomposites with enhanced photocatalytic activities. *J. of Nanoparticle Res.*, 27(2), 49. DOI: 10.1007/s11051-025-06242-0
- Hudlikar, M., Joglekar, S., Dhaygude, M. and Kodam, K. (2012). Green synthesis of TiO<sub>2</sub>nanoparticles by using aqueous extract of *Jatropha curcas* L. latex. *Materials Letters*, 75, 196–199. DOI: 10.1016/j.matlet.2012.02.018
- Iravani, S. (2011). Green synthesis of metal nanoparticles using plants. *Green Chemistry*, 13(10), 2638–50. DOI: 10.1039/c1gc15386b
- Kandregula, G. R. (2015). Green synthesis of TiO<sub>2</sub>nanoparticles using aloe vera extract. *International Journal of Advanced Research in Physical Science* 2, 28–34.
- Nadaroğlu, H., Güngör, A. A. and İnce, S. (2017). Synthesis of nanoparticles by green synthesis method. *International Journal of Innovative Research and Reviews*, 1(1), 6–9.
- Nainani, R., Thakur, P. and Chaskar, M. (2012). Synthesis of silver doped TiO<sub>2</sub> nanoparticles for the improved photocatalytic degradation of methyl orange. *Journal of Materials Sciences and Chemical Engineering*, 2(1), 52–58.
- Godbert, N., Mastropietro, T. and Poerio, T. (2018). *Mesoporous TiO<sub>2</sub> Thin Films: State of the Art*. DOI: 10.5772/intechopen.74244
- Peralta-Videa, J. R., Huang, Y., Parsons, J. G., Zhao, L., Lopez-Moreno, L., Hernandez-Viezcas, J. A. and Gardea-Torresdey, J. L. (2016). Plant-based green synthesis of metallic nanoparticles: Scientific curiosity or a realistic alternative to chemical synthesis. *Nanotechnology for Env. Engr.*, 1(1), 4. DOI: 10.1007/s41204-016-0004-5
- Periyat, P., Pillai, S. C., McCormack, D. E., Colreavy, J. and Hinder, S. J. (2008). Improved high-temperature stability and sun-light-driven photocatalytic activity of sulfur-doped anatase TiO<sub>2</sub>. *The Journal of Physical Chemistry C*, 112(20), 7644–52. DOI: 10.1021/jp0774847

- Raghunandan, D., Bedre, M. D., S. Basavaraja, Sawle, B., Manjunath, S. Y. and Venkataraman, A. (2010). Rapid biosynthesis of irregular shaped gold nanoparticles from macerated aqueous extracellular dried clove buds (*Syzygium aromaticum*) solution. *Colloids and Surfaces. B, Biointerfaces*, 79(1), 235–40. DOI: 10.1016/j.colsurfb.2010.04.003
- Rauwel, P., Rauwel, E., Ferdov, S. and Singh, M. (2015). Silver nanoparticles: Synthesis, properties and applications. *Journal of Advances in Materials Sciences and Engineering*, Article 624394. DOI: 10.1155/2015/624394
- Raveendran, P., Fu, J. and Wallen, S. L. (2003). Completely green synthesis and stabilization of metal nanoparticles. *Journal of the American Chemical Society*, 125(46), 13940–41. DOI: 10.1021/ja029267j
- Sellami, H., Akinyemi, M. O., Maroua Gdoura-Ben Amor, Onwudiwe, D. C. and Mthiyane, D. M. N. (2025). Structural and optical characterization of TiO<sub>2</sub> nanoparticles synthesized using globularia alypum leaf extract and the antibacterial properties. *Discover Applied Sciences*, 7, 834. <https://doi.org/10.1007/s42452-025-07521-0>
- Sethy, N. K., Arif, Z., Mishra, P. K. and Kumar, P. (2020). Green synthesis of TiO<sub>2</sub> nanoparticles from syzygium cumini extract for photo-catalytic removal of lead (Pb) in explosive industrial wastewater, 171–81.
- Singh, T., Singh, V., Wang, W., Yadav, D., Kumar, A. and Singh, P. K. (2019). Biosynthesized nanoparticles and its implications in agriculture. pp. 257–74. DOI: 10.1201/9780429265235-19
- Smith, A. M., Duan, H., Rhyner, M. N., Ruan, G. and Nie, S. (2006). A systematic examination of surface coatings on the optical and chemical properties of semiconductor quantum dots. *Physical Chemistry Chemical Physics: PCCP* 8(33), 3895–3903. DOI: 10.1039/b606572b
- Subhapriya, S. and Gomathipriya, P. (2018). Green synthesis of titanium dioxide (TiO<sub>2</sub>) nanoparticles by trigonella foenum-graecum extract and its antimicrobial properties. *Microbial Pathogenesis*, 116, 215–20. <https://doi.org/10.1016/j.micpath.2018.01.027>
- Sundrarajan, M. and Gowri, S. (2011). Green synthesis of titanium dioxide nanoparticles by nyctanthes arbor-tristis leaves extract. *Chalcogenide Letters*, 8(8), 447–451.